Palladium on S,N-Containing Carbon Materials Derived from Covalent Triazine-Based Frameworks (CTF) for C-C Coupling and Electrocatalytic Hydrogen Production

Arijit Maity, [a] Debabrata Patra, [b] Dr. Amit Saha, [b] and Asamanjoy Bhunia*[a]

[a]Department of Chemistry, Inorganic Chemistry Section, Jadavpur University, Kolkata 700032, India.
E-mail: abhunia.cheistry@jadavpuruniversity.in

[b]Department of Chemistry, Organic Chemistry Section, Jadavpur University, Kolkata 700032, India

Materials

All chemicals were purchased from commercial suppliers (Sigma-Aldrich, Acros Organics, and TCI chemical company) and used without further purification. The monomer 2, 3, 6, 7-tetra (4-cyanophenyl) tetrathiafulvalene (TTF-CN) was synthesized following previously reported procedures.[1]

Analytical Techniques

Infrared (IR) spectra were obtained on a Bruker FT-IR Tensor 37 spectrometer in the 4000–550 cm^{-1} region with 2 cm^{-1} resolution as KBr disks. NMR experiments were performed on Bruker DPX300 spectrometers at 298 K. The manufacturers' supplied Bruker TopSpin 3.6.2 software was utilized to process the data. NMR chemical shifts were recorded in δ ppm by locking and calibration with appropriate deuterated NMR solvents. Elemental analyses were carried out using a PerkinElmer 2400 series II elemental analyzer. Powder X-ray diffraction (PXRD) data were collected on a Bruker D2 Phaser diffractometer using a flat sample holder, including flat silicon, low background sample holder, and Cu $K\alpha_1/\alpha_2$ radiation with λ = 1.5418 Å at 30 kV covering 2theta angles 5–80° over a time of 2 h (0.01° sec^{-1}). Diffractograms were obtained on flat layer sample holders where at a low angle the beam spot is strongly broadened so that only a fraction of the reflected radiation reaches the detector which leads to low relative intensities measured at $2\theta < 7°$. For hygroscopic or air-sensitive samples, the sample holder can be sealed with a dome. Scanning electron microscopy (SEM) images were obtained using an ESEM Quanta 400 FEG SEM equipped with a secondary electron detector. Thermogravimetric analyses (TGA) were carried out at a ramp rate of 10 °C min^{-1} under N_2 flow with a Netzsch TG 209 F3 Tarsus. Nitrogen physisorption isotherms were carried out on a Nova 4000e from Quantachrome at 77 K (liquid nitrogen bath) using N_2 gas of 99.99% purity. The sample was connected to the preparation port of the sorption analyzer and degassed under vacuum until the outgassing rate, *i.e.*, the rate of pressure rises in the temporarily closed manifold with the connected sample tube, was less than 2 μTorr min^{-1} at a specified temperature of 130 °C. After weighing, the sample tube was then transferred to the analysis port of the sorption analyzer. Helium gas was used for the determination of the cold and warm free space of the sample tubes. The DFT pore size distributions ('N_2 DFT slit pore' model) were calculated using the NovaWin 11.03' software. X-ray photoelectron spectroscopy (XPS) measurement was conducted using the Thermo Fisher ESCALAB Xi+ microProbe instrument with a monochromatic Al–Kα target, 1486.6 eV energy, and a maximum power of 15.0 kW. The high-resolution transmission

electron microscopy (HRTEM) images were collected from the JEOL, JEM-2100F instrument, operating at an accelerating voltage of 200 kV. Before the analysis, the 2- propanol solution of a small amount of sample was dispersed homogeneously in an ultrasonic cleaner for 2h to ensure maximum dispersion of the sample, and then 2 µL of the solution was cast on a carbon coated Cu-grid (300 mesh size), put in an airtight desiccator, and dried at ambient temperature for two days. The leached out palladium during C-C coupling reaction was measured by Inductively coupled plasma optical emission spectrometry (ICP-OES) from an Icap 7000 ICP-OES (Thermo Scientific). For leaching test, we performed four consecutive catalytic cycles and collected the filtrate after each cycle. The combined filtrates were evaporated to dryness, and the residual solid was digested in 3% HNO_3 to obtain a solution suitable for ICP–OES analysis. Even after five successive runs, the cumulative amount of palladium leached was limited to 0.123 mg/L.

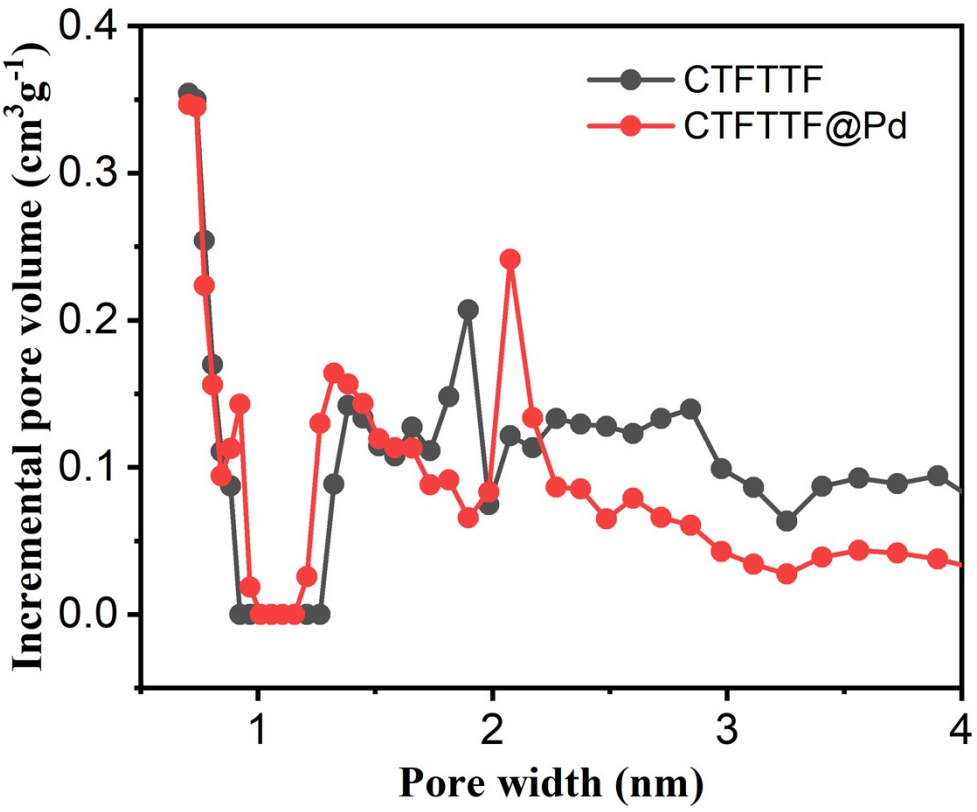

Fig. S1: Pore size distribution Curve.

Table S1: Surface area of CTFTTF and CTFTTF@Pd.

CTFs	$S_{BET}(m^2g^{-1})$	$S_{Lang}(m^2g^{-1})$	$V_{0.1}(cm^3g^{-1})$	$V_{Total}(cm^3g^{-1})$	$V_{0.1}/V_{Total}$
CTFTTF	650	926	0.24	0.68	0.35
CTFTTF@Pd	422	855	0.18	0.48	0.31

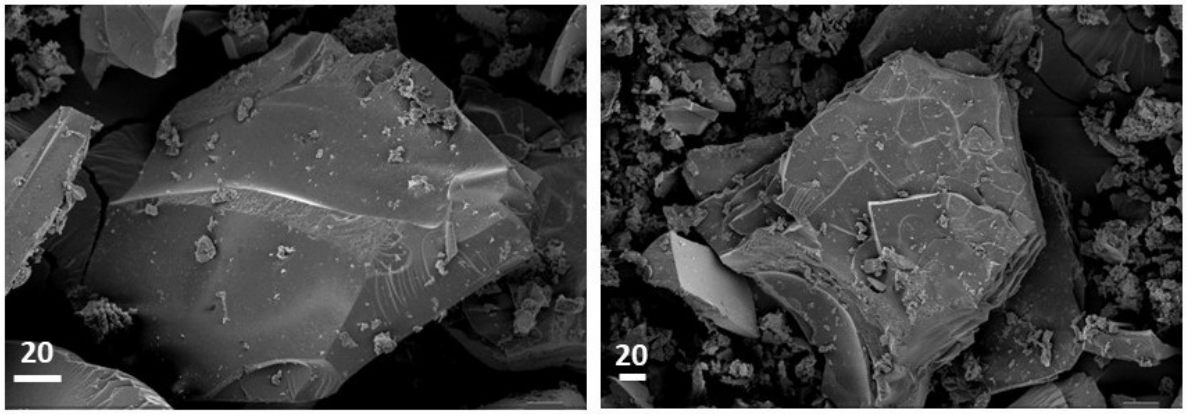

Table S2: The % of weight and % of atom present in CTFTTF@Pd found from EDX.

Element	Weight %	Atomic %	Net Int.
C K	56.28	66.45	1064.16
N K	30.11	30.47	142.83
S K	4.09	1.81	374.72
Pd L	9.52	1.27	367.69

Fig. S2: SEM images of CTFTTF. The length of the scale bar is given in µm.

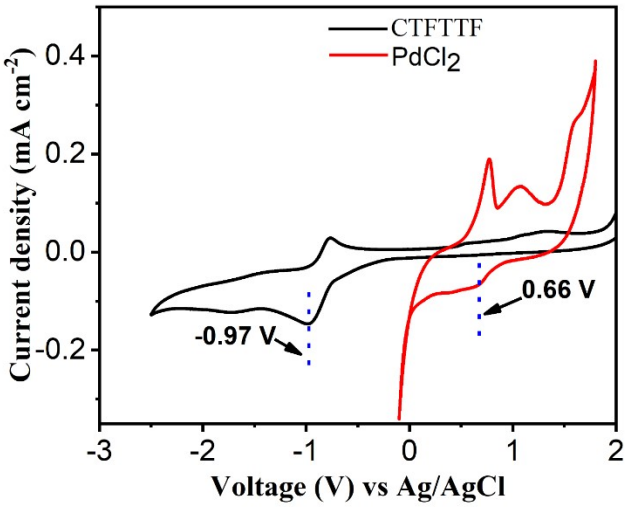

Fig. S3: CV of CTFTTF and $PdCl_2$ in 0.1M tetrabutylammonium hexafluorophosphate solution.

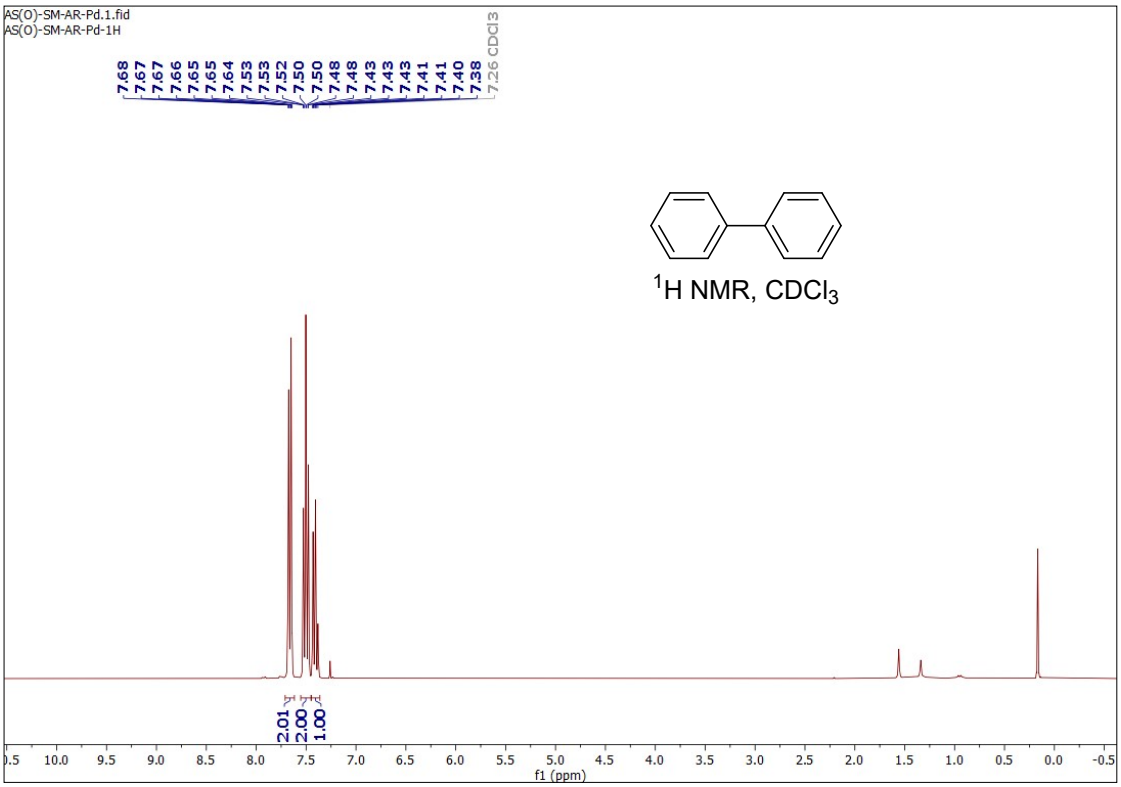

Fig. S4: ^{1}H NMR spectrum (300 MHz) of compound **1** in $CDCl_3$.

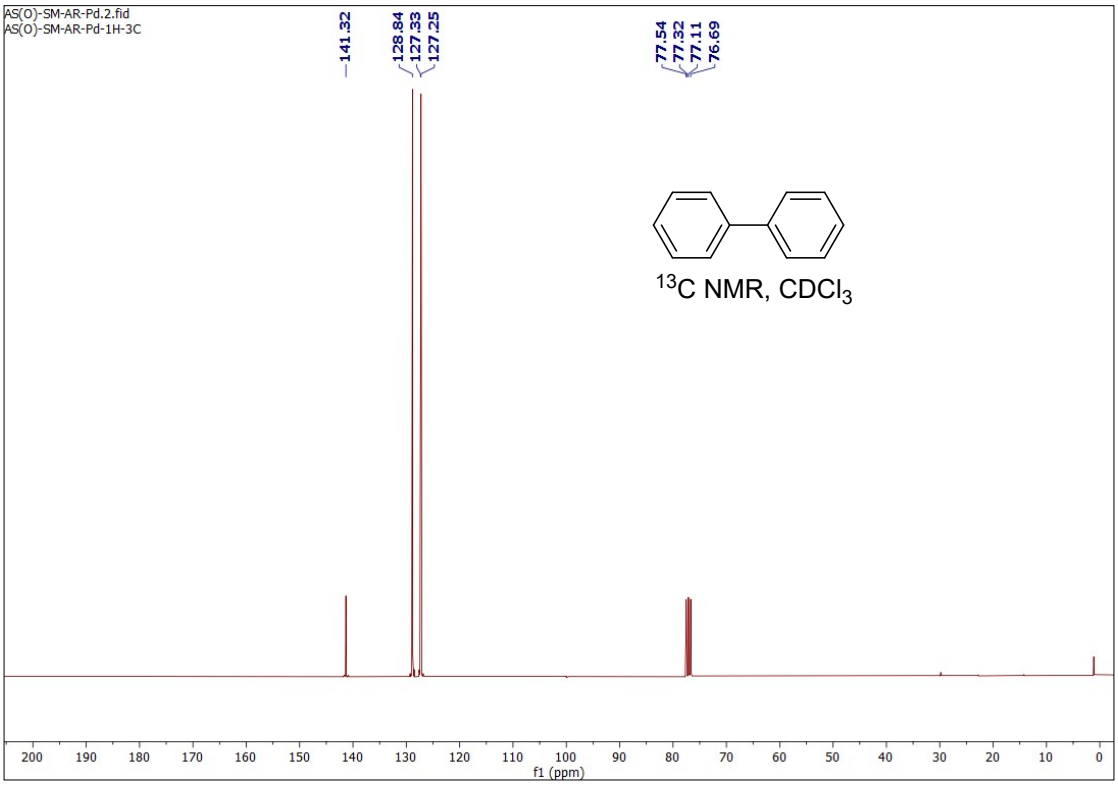

Fig. S5: ^{13}C NMR spectrum (75 MHz) of compound **1** in $CDCl_3$.

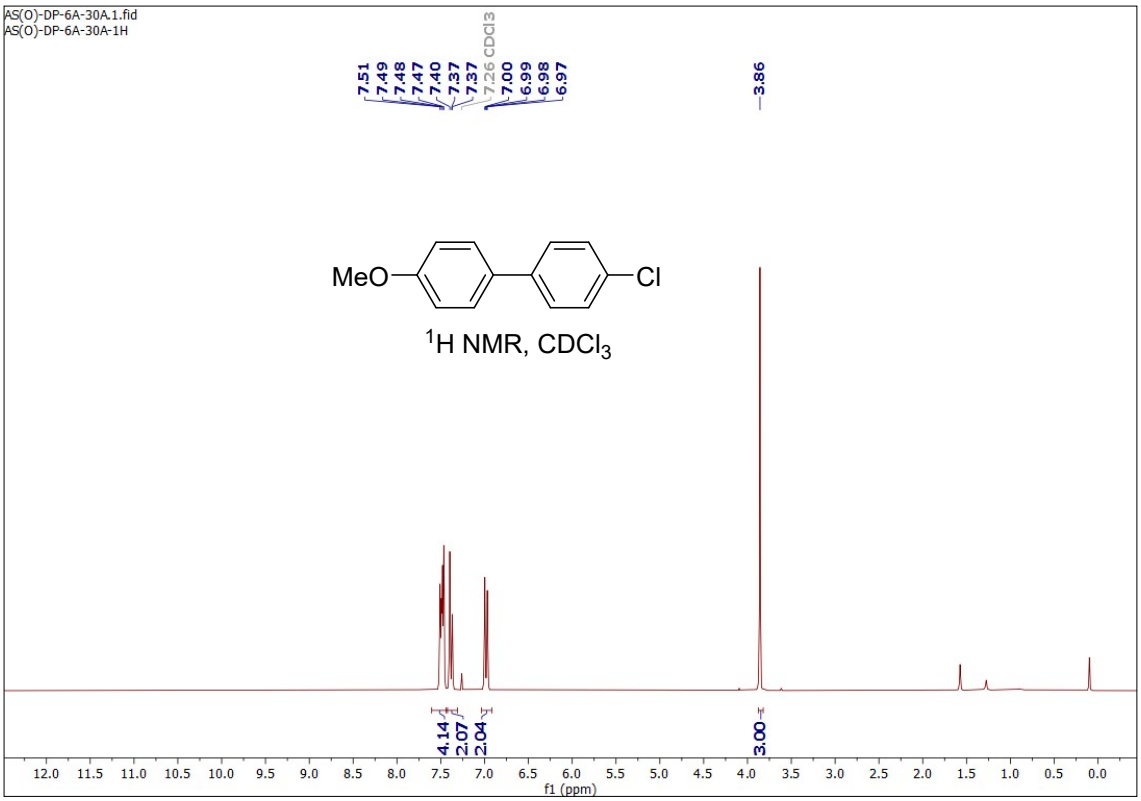

Fig. S6: ^{1}H NMR spectrum (300 MHz) of compound **2** in $CDCl_3$.

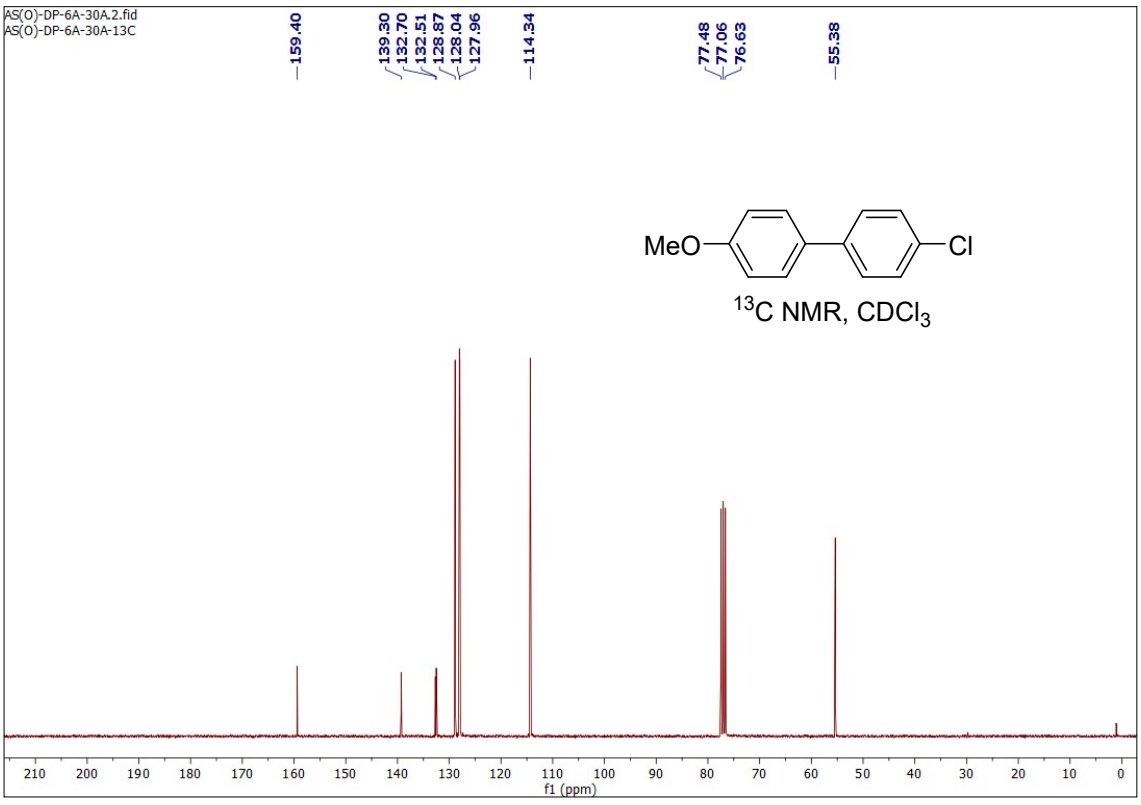

Fig. S7: ^{13}C NMR spectrum (75 MHz) of compound **2** in $CDCl_3$.

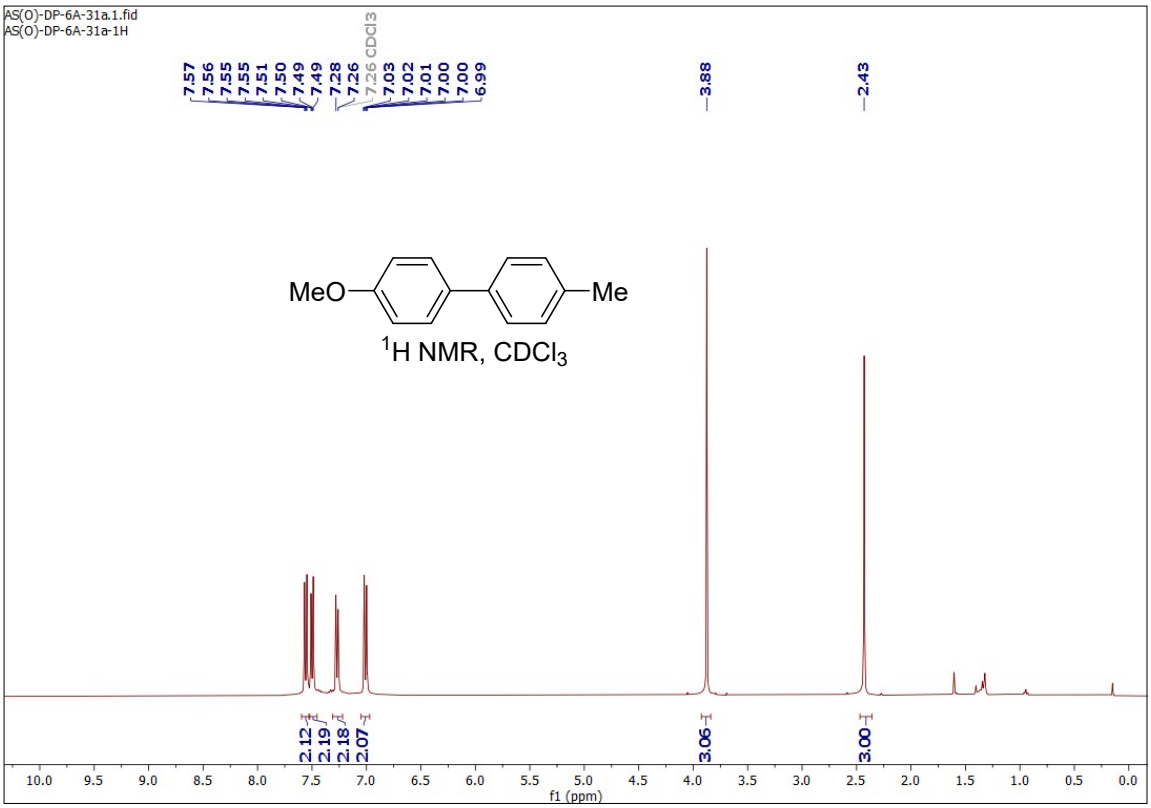

Fig. S8: ^{1}H NMR spectrum (300 MHz) of compound **3** in $CDCl_3$.

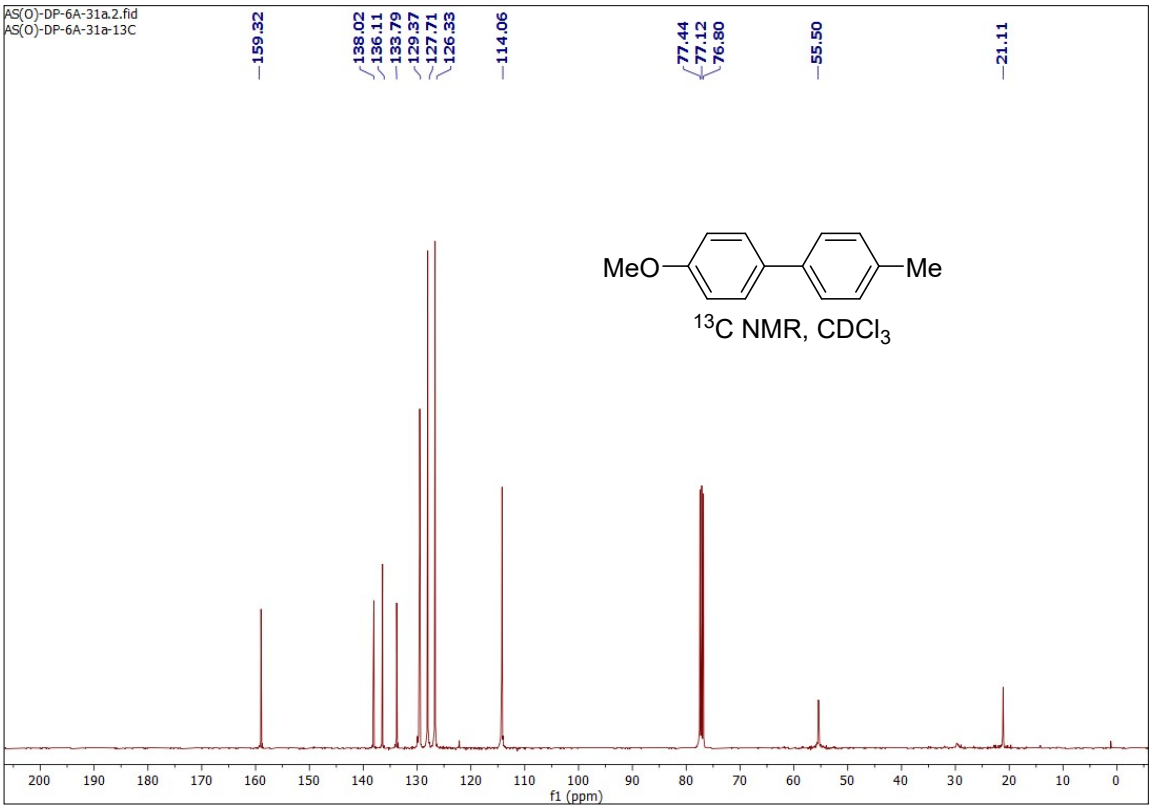

Fig. S9: ^{13}C NMR spectrum (75 MHz) of compound **3** in $CDCl_3$.

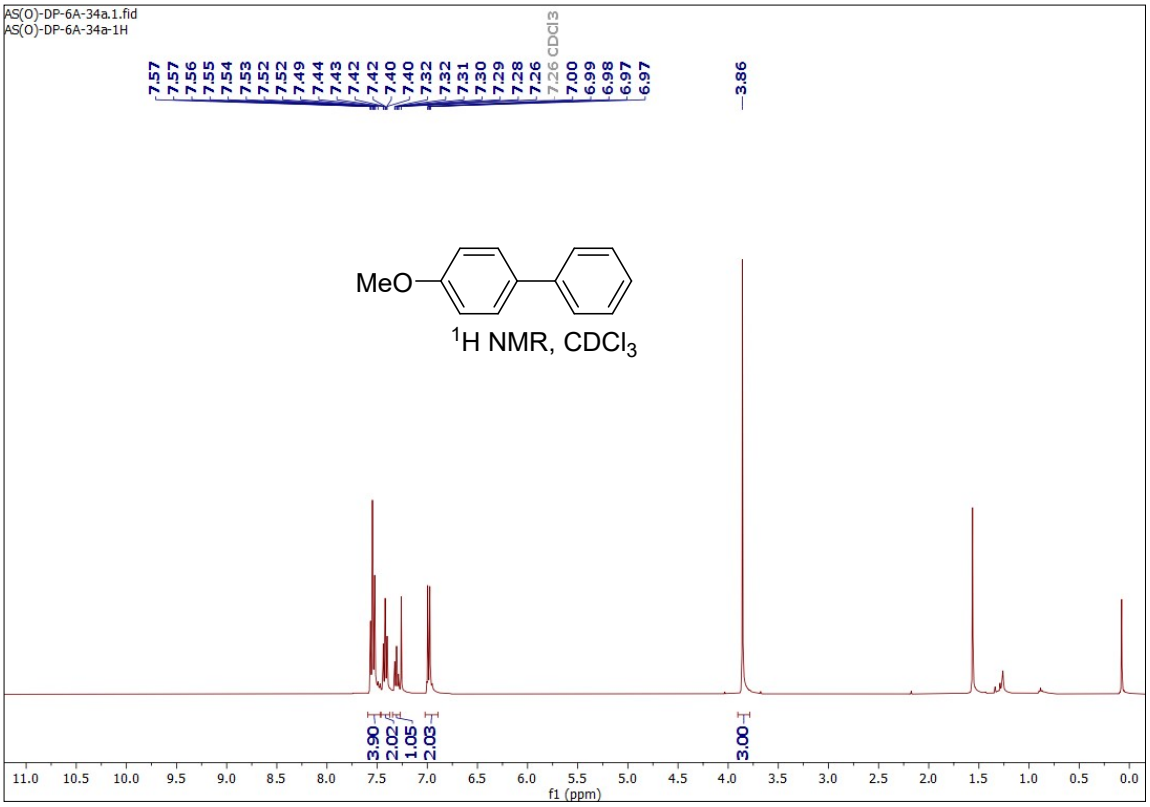

Fig. S10: ^{1}H NMR spectrum (300 MHz) of compound **4** in $CDCl_3$.

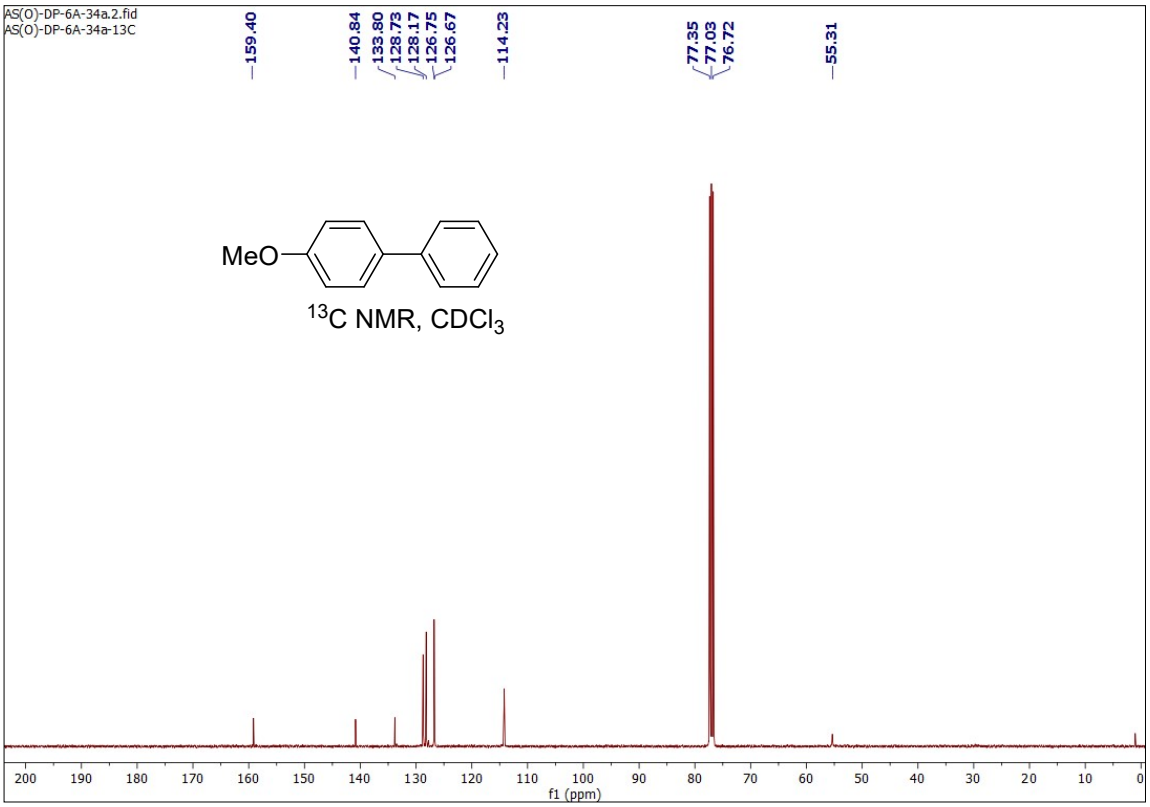

Fig. S11: ^{13}C NMR spectrum (75 MHz) of compound **4** in $CDCl_3$.

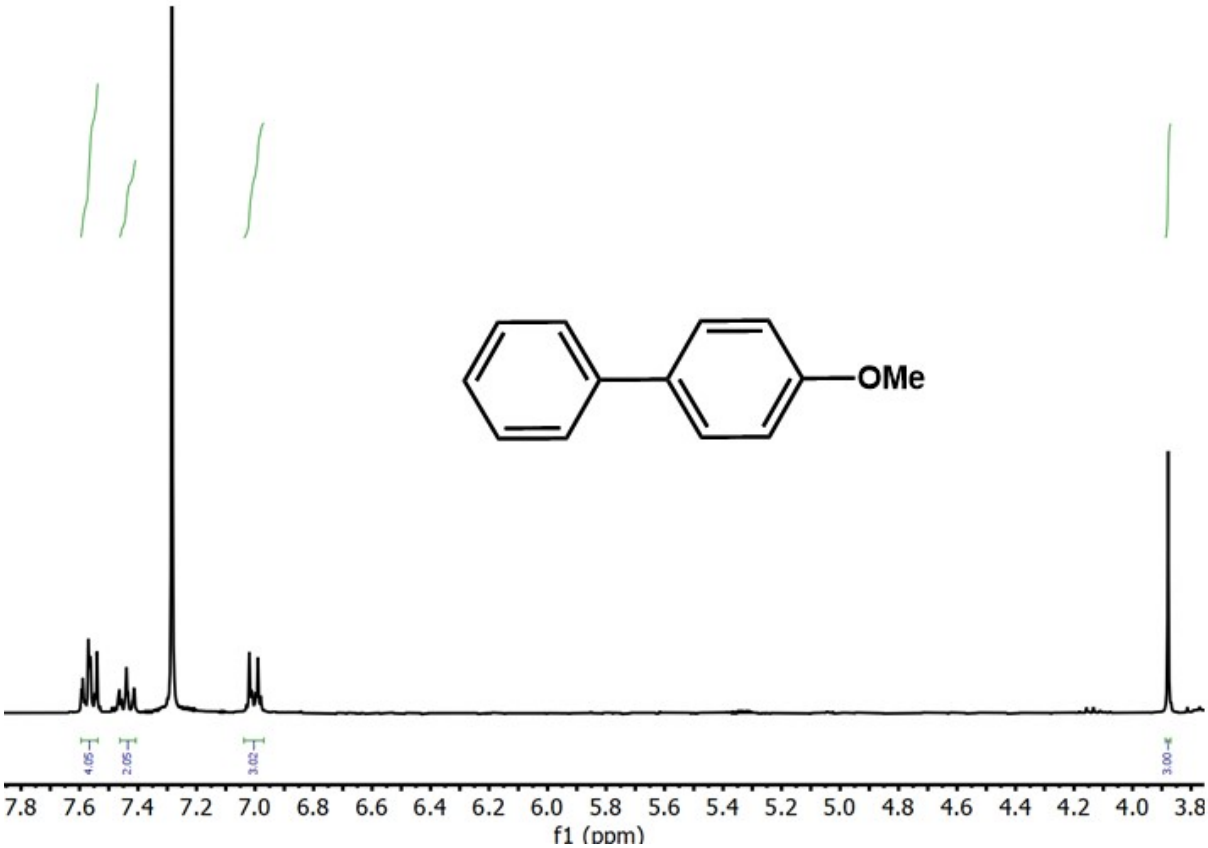

Fig. S12: ^{1}H NMR spectrum (300 MHz) of compound **4** in $CDCl_3$

Table S3: Comparison of the Catalytic Activities of Different Catalysts of Suzuki–Miyaura cross-coupling reaction.

SL No	Catalyst	Temp. (°C)	Solvent	Time(h)	Yield (%)	Stability (runs)	Ref.
1.	Pd^{II}/TAT–DHBD	120	DMF	24	56	—	[2]
2.	Pd^{0}/TAT–DHBD	120	DMF	24	62	—	
3.	Pd^{II}/TAT–TFP	120	DMF	24	80	5	1
4.	Pd^{0}/TAT–TFP	120	DMF	24	83	5	1
5.	TAPB–BTCA	80	THF	2	51	—	[3]

6.	(Pd/C)@TpPa	30	EtOH/H_2O	24	87	5	[4]
7.	Pd/COF-SMC2	150	xylene	3	47	4	[5]
8.	Pd@TAPB-BTCA	80	THF	3	70	—	[6]
9.	Pd/COF-BASU1	110	DMF	1	80	5	[7]
10.	Pd@COF-Me	50	H_2O	6	79	10	[8]
11.	Pd/COF-LZU1	150	p-Xylene	3	97	5	[9]
12.	PdNPs@Thio-COF	50	DMF/H_2O	3	85	5	[10]
13.	Pd@TPM-3D-COF-Bpy	70	DMF/H_2O	5	98	5	[11]
14.	CTFTTF@Pd	60	DMF	12	68-78	4	**This Work**

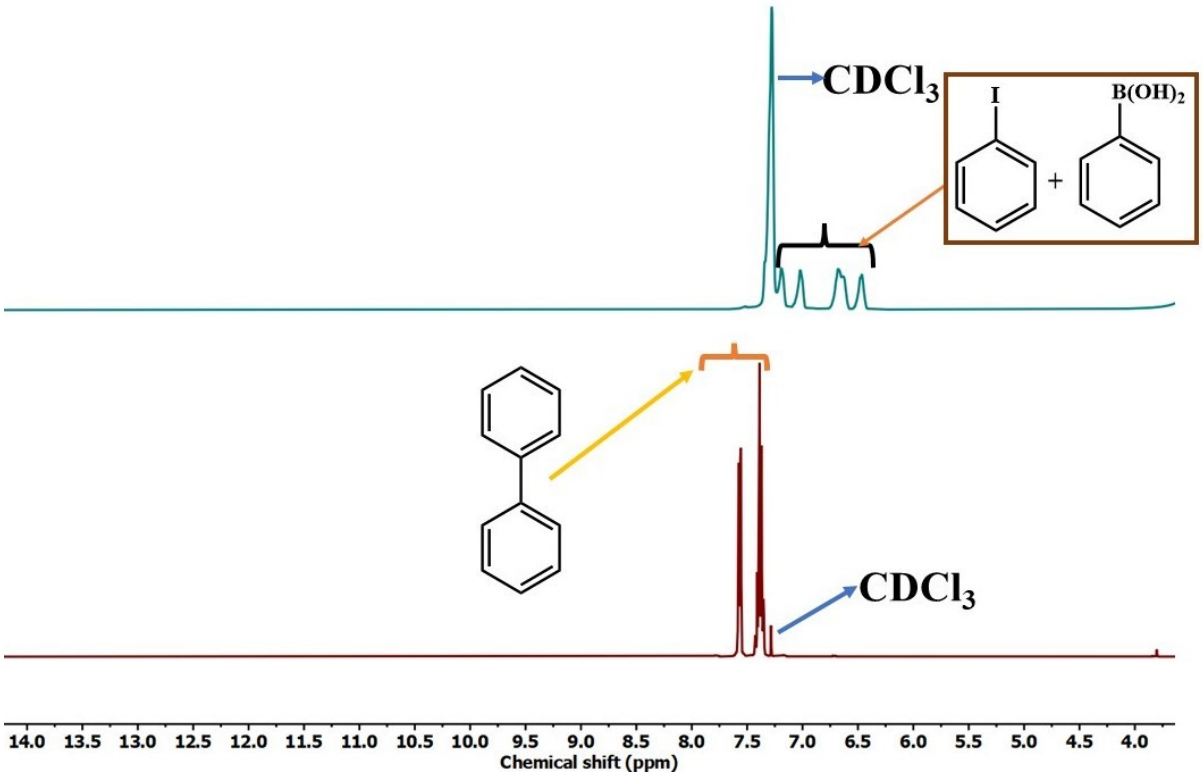

Fig. S13: ^{1}H NMR spectra in $CDCl_3$. The upper (blue colour) ^{1}H NMR spectrum represents the crude product, which is isolated after the reaction during leaching test. The lower spectrum (brown colour) represents the reaction in the presence of the catalyst. As the two spectra are not similar, we can conclude that there was no leaching of the catalyst.

Table S4: (a) Catalytic Activities of CTFTTF@Pd of Suzuki–Miyaura Cross-Coupling Reaction

Catalyst	Reactant-1	Reactant-2	Product	Yield (%)	TON
CTFTTF@Pd	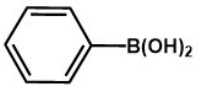	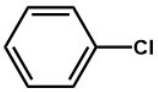	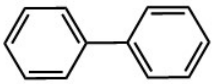	0	0
	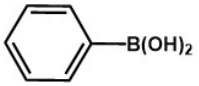	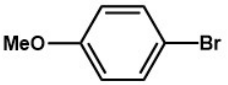	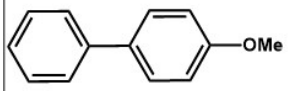	10	8.47
	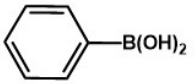	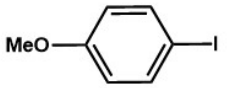	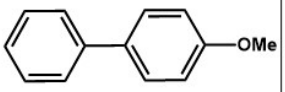	70	59.32

Table S4: (b) Catalytic Activities of CTFTTF@Pd of Suzuki–Miyaura Cross-Coupling Reaction

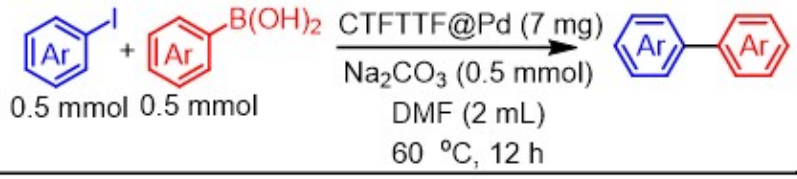

Entry	Ar-I	Ar-B(OH)$_2$	Product	Yield (%)	TON
1	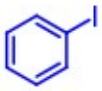	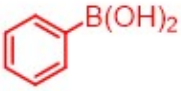	 **1**	78	66.10
2	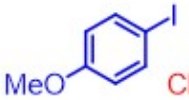	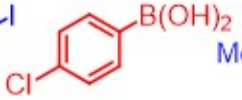	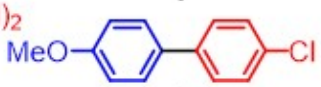 **2**	70	59.32
3	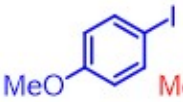	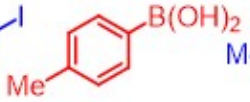	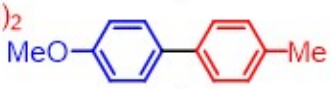 **3**	72	61.00
4	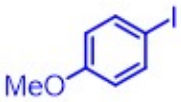	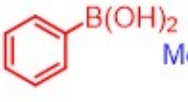	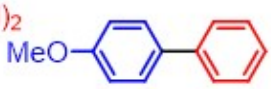 **4**	70	59.32
5	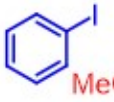	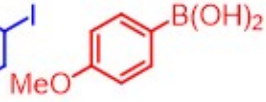	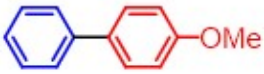	68	57.62

Reaction condition: A mixture of Ar-I (0.5 mmol), Ar-B(OH)$_2$ (0.5 mmol), Na_2CO_3 (0.5 mmol) and CTFTTF@Pd catalyst (7 mg) in 2 mL of DMF was stirred for 12 h at 60 °C. Yields represent the isolated yield.

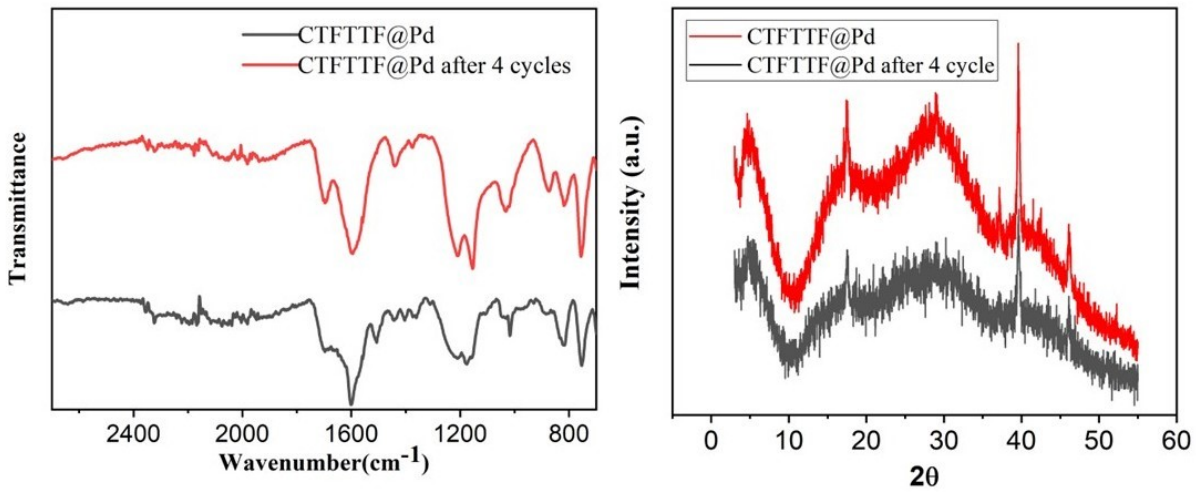

Fig. S14: IR spectra (left side) and PXRD spectra (right side) of CTFTTF@Pd after catalysis (four cycles).

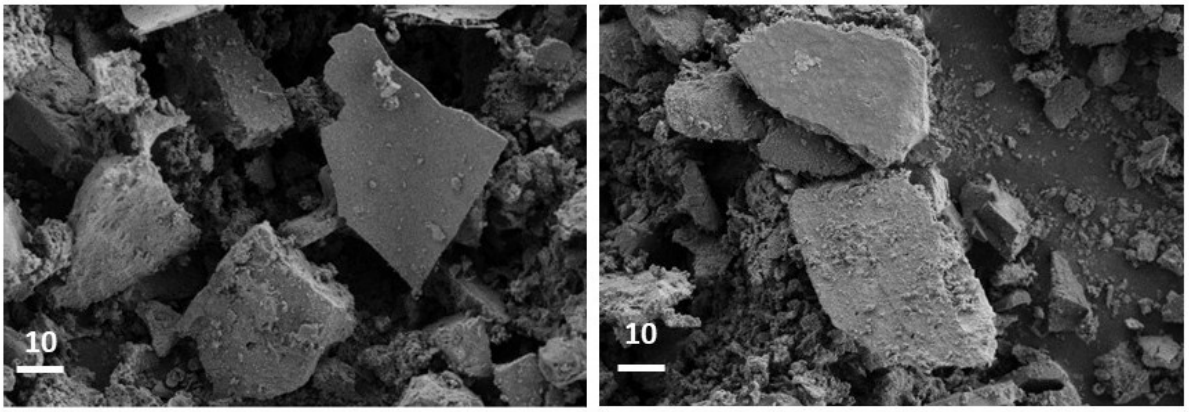

Fig. S15: SEM images of CTFTTF@Pd after catalysis (four cycles). The length of the scale bar is given in µm.

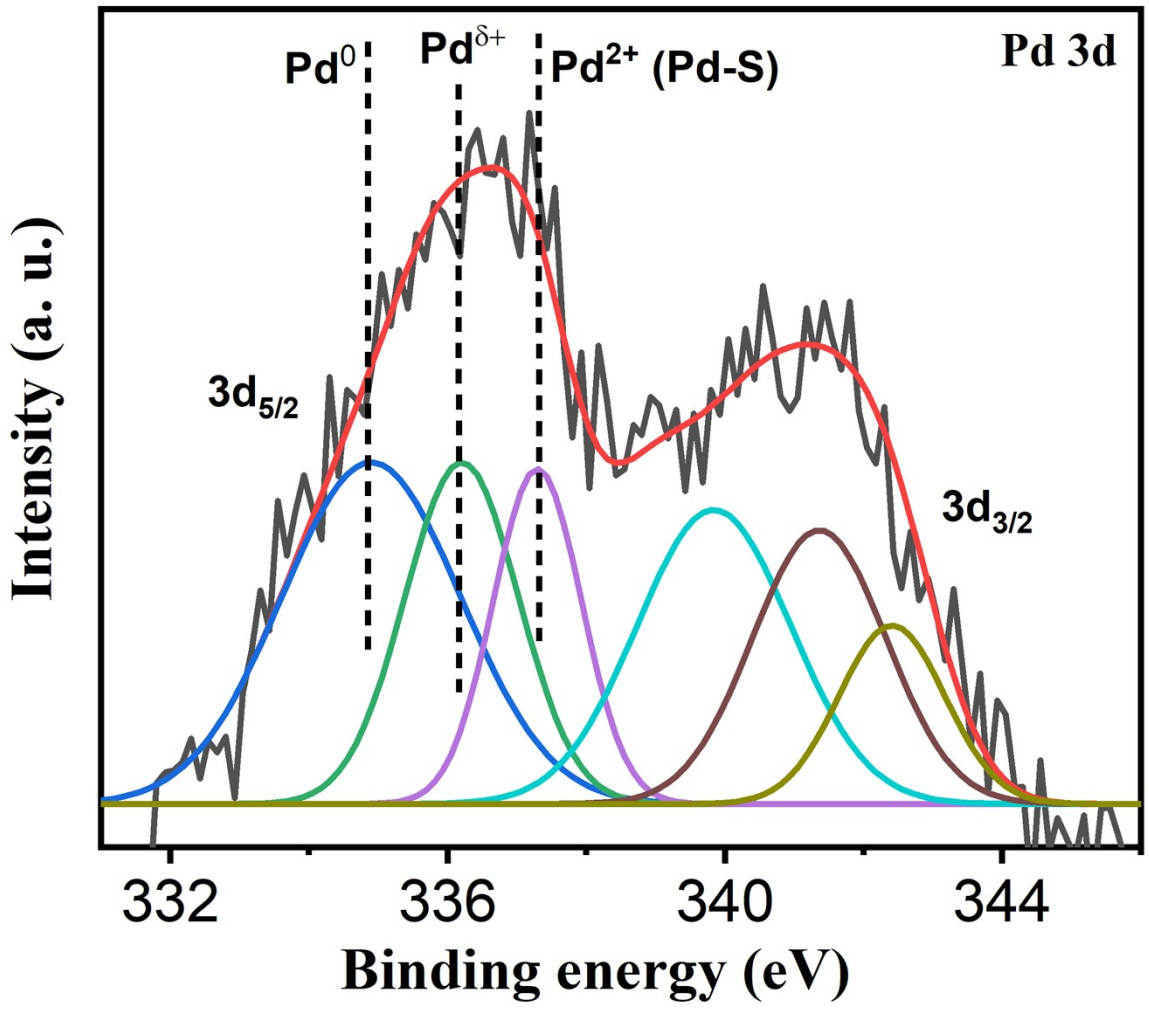

Fig. S16: XPS of CTFTTF@Pd for Pd 3d.

Electrochemical measurements

Electrode preparation

Electrochemical measurement was performed using a computerized CHI 760E electrochemical workstation with a three-electrode system. In this study, the platinum electrode, Ag/AgCl electrode and glassy carbon electrode are acted as counter electrode, reference electrode and working electrode, respectively. The geometric area of the electrode (0.071 cm2). The catalyst ink was prepared by taking 4.0 mg of catalyst in the solution of 400 µL of HPLC grade IPA and 40 µL of 5 wt% Nafion. Then it was sonicated for 15 min. After that, the prepared catalyst ink was deposited on a glassy carbon working electrode. The geometric area of the electrode is 0.071 cm^2. The catalyst loading on the surface of the glassy carbon electrode (GCE) was 0.8 mg for CTFTTF@Pd and 0.7 mg for CTFTTF@Pd-R, respectively. The 1.0 M KOH solution (pH 14.0) was utilized as the electrolyte solution. Nitrogen gas was purged for 15 min before every electrochemical measurement. The LSV measurements were carried out with a scan rate of 10 mV/s. EIS was performed in a frequency range from 1 to 10^5 Hz. All samples were measured twice to ensure reproducibility.

For bulk electrolysis experiments, graphite plates were cut into 2 × 1 cm^2 slides and thoroughly cleaned by sequential sonication in deionized water, ethanol, and acetone. After drying, the catalyst ink was uniformly deposited onto the cleaned graphite plates and allowed to dry before use in bulk electrolysis measurements. The catalyst loading of CTFTTF@Pd-R on the graphite paper electrode was 4 mg.

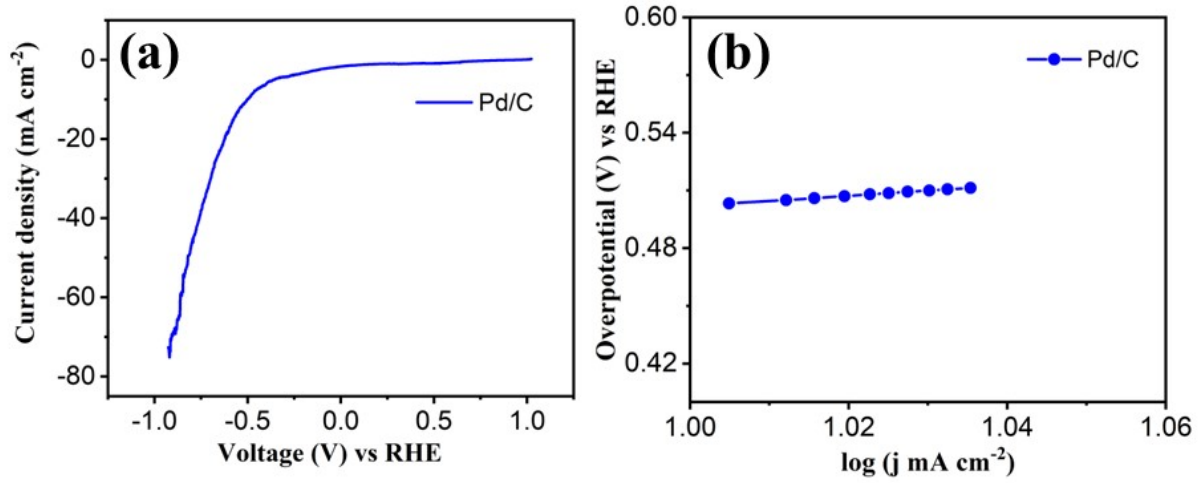

Fig. 17: (a) LSV curve (b) Tafel slope of Pd/C.

Table S5: Overpotential and Tafel slope of Pd/C, CTFTTF@Pd and CTFTTF@Pd-R for HER activity.

Ctalyst	Overpotential (mV)	Tafel Slope (mV $dec^{-1)}$

Pd/C	309	267
CTFTTF@Pd	755	249
CTFTTF@Pd-R	600	144

Table S6: Comparison of the Catalytic Activities of Different Catalysts of Electrocatalytically hydrogen evolution reaction.

SL No	Catalyst	Pd loading	TON / TOF	HER Overpotential (mV)	Tafel slope (mV dec^{-1})	Ref
1.	PY- SE–COF–Pd	16.8 Wt%	—	128	150	[12]
2.	PdKMX	1.10 wt%	0.326 s^{-1}	72	69	[13]
3.	porous Pd-CNx	59.4 Wt %	—	55	35	[14]
4.	Pd/g-C_3N_4	32.98 Wt %	—	105	69	[15]
5.	Pd-CoCNT	—	—	112	56	[16]
6.	Pd/3D-N-rGO	86.3 Wt%	—	92.9	136	[17]
7.	Pd@CNT	42.82 Wt % w/w	—	127	41	[18]
8.	Pd/NF	0.45 mg	—	125	83	[19]
9.	Pd-NC	37.3 Wt %	—	84	136	[20]
10.	rGO-PdPS	—	0.3 s^{-1}	100	46	[21]
11.	Pd@NDCD	—	—	291	135	[22]
12	CTFTTF@Pd-R	9 wt %	3.6 s^{-1}	600	144	**This work**

Calculations

1. Electrochemical double-layer capacitance (C_{dl})

Electrochemical double layer capacitance for the CTFTTF@Pd and CTFTTF@Pd-R were determined by measuring the current in the non-faradic region through CV at different scan rates in the voltage window of -1 to 1 V (V vs. RHE), followed by plotting a graph between

scan rate and current at the mid-point of the potential window and subsequently linear fitting the curve to obtain the slope, i.e., double layer capacitance[23]. This non-faradic region is typically a 0.2 V window about the open circuit potential, and all the measured current values are due to double-layer charging[24]. The double-layer capacitance (C_{dl}) was calculated using the equation given below:

$i_c = v\ C_{dl}$..... **equation S1**

Where,

i_c = Double-layer charging current

v = Scan rate

2. Electrochemically active surface area (ECSA)

Electrochemically active surface area (ECSA) for the CTFTTF@Pd and CTFTTF@Pd-R was calculated.

The ECSA was calculated using the equation given below:

$$ECSA = \frac{C_{dl}}{C_s} \quad \text{..... equation S2}$$

Whereas, C_{dl} = Double-layer capacitance and C_s = specific capacitance of the system (constant factor).

The value of specific capacitance for the flat surface electrode/catalyst in an alkaline medium[25] is usually 0.036 mF/cm^2. The unit of ECSA is per cm^2.

3. **Roughness Factor (RF)**

The roughness factor for the CTFTTF@Pd and CTFTTF@Pd-R is calculated by the following equation:

$$RF = \frac{ECSA}{Electrode\ geometrial\ area} \quad \text{..... equation S3}$$

There is no unit of roughness factor.

4. **Mass activity**: Mass activity was calculated using the following equation[26].

$$Mass\ activity\ (A\ g^{-1}) = \frac{j\ (A\ cm^{-2})}{Mass\ \ (g\ cm^{-2})} \quad \text{..... equation S4}$$

Where, j = current density, m = mass loading

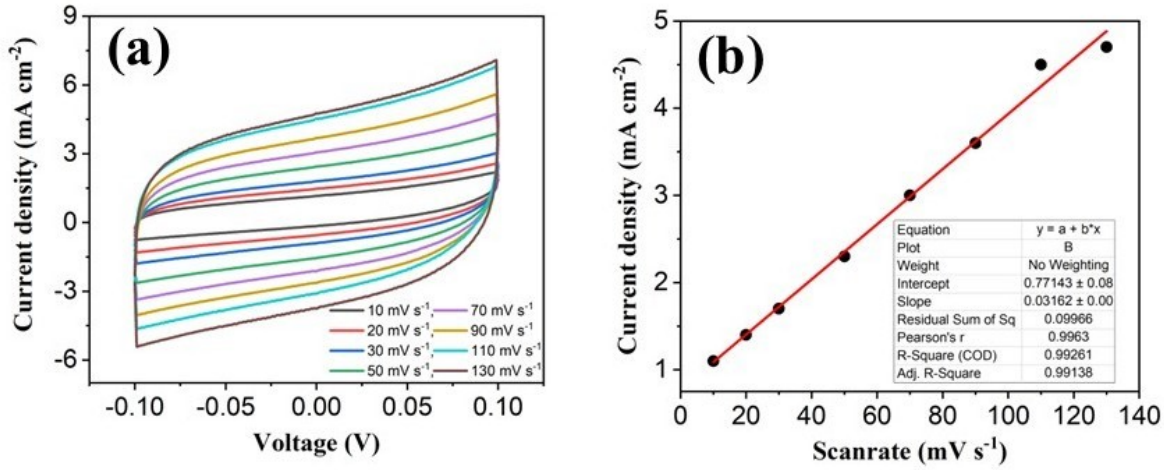

Fig. S18: (a) Electrochemical double-layer capacitance acquired from the CV curves in the non-Faradaic region of CTFTTF@Pd in N_2-saturated 1 M aqueous KOH (b) Current as a function of scan rates of CTFTTF@Pd obtained from Fig. S18(a).

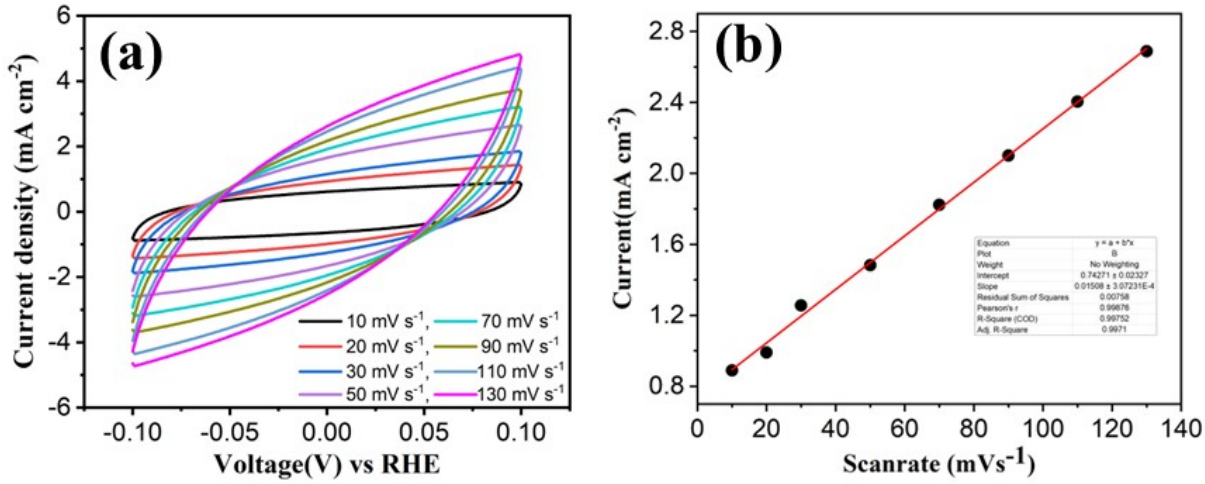

Fig. S19: (a) Electrochemical double-layer capacitance acquired from the CV curves in the non-Faradaic region of CTFTTF@Pd in N_2-saturated 1 M aqueous KOH (b) Current as a function of scan rates of CTFTTF@Pd obtained from S19(a).

Table S7: Performance parameters of CTFTTF@Pd for HER

Parameter	CTFTTF@Pd	CTFTTF@Pd-R
Overpotential	755 mV	600 mV

Tafel Slope	249 mV dec^{-1}	144 mV dec^{-1}
Double layer capacitance (C_{dl})	7.58 mF/cm^2	15.75 mF/cm^2
Electrochemical active surface area (ECSA)	13.45 cm^2	27.95 cm^2
Roughness factor (R_f)	189.43	393.66

Determination of FE:

H_2 produce for CTFTTF@Pd-R coated graphite plate in CPE is 1.1 mL.

Amount of H_2 produced for blank graphite plate is 0.4 mL

The amount of hydrogen produce only for catalyst = (1.1 - 0.4) = 0.7mL

Mol of hydrogen produce = 0.7/22400 mol

$$FE = \frac{2 \times mol\ of\ Hydrogen\ produce \times 96500}{Total\ charge} \times 100 \ldots\ldots\ldots\ldots\ldots\ldots\ldots \textbf{equation S5}$$

$$= \frac{2 \times 0.7/22400 \times 96500}{8.29}$$

= 72.75%

Determination of TOF:

For TOF (s^{-1}) calculation, CV scans from -0.2 to +0.6 V versus RHE were carried out in 1 M PBS at 50 mV s^{-1} (Figure). The TOF values were calculated according to Equations (S6), (S7) and (S8) (assuming one electron change during both oxidation and reduction process)

$$TOF = \frac{I}{2nF} \ldots\ldots\ldots\ldots\ldots \textbf{equation S6}$$

where I, n and F represent the current (A) during LSV measurements in 1M KOH solution, number of active sites (mol) and Faraday constant (96500 C mol-1), respectively.

$$n = \frac{Q}{2F} \ldots\ldots\ldots \textbf{equation S7}$$

Q is the voltammetric charge (C); ν refers to the scan rate (V s^{-1}).

$$Q = \frac{Intregrated\ CV\ area}{\nu}$$

From the above equations, we come to conclusion the following equation

$$TOF = \frac{I}{Q} \ldots\ldots\ldots\ldots\ldots \textbf{equation S8}$$

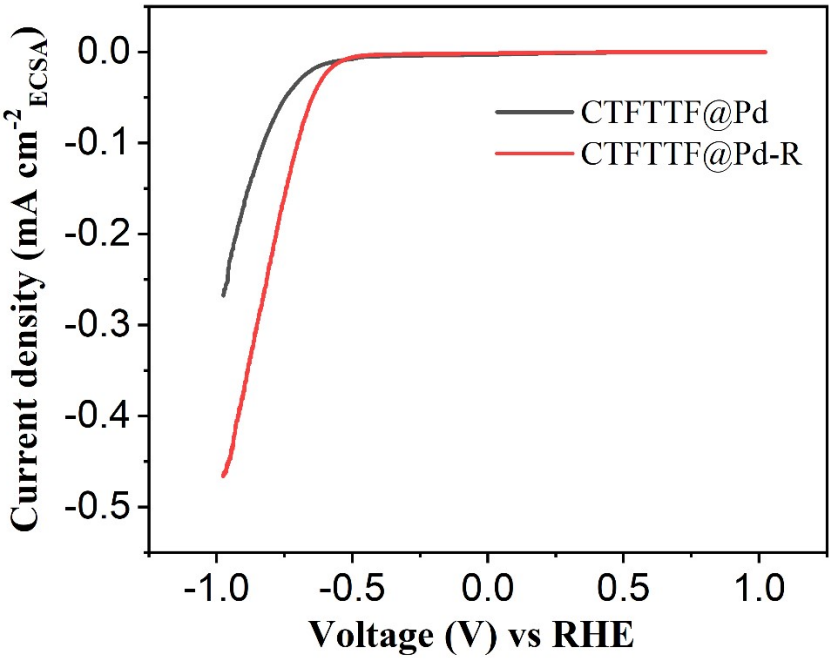

Fig. S20: ECSA normalized LSV polarization curves for electrocatalytic HER.

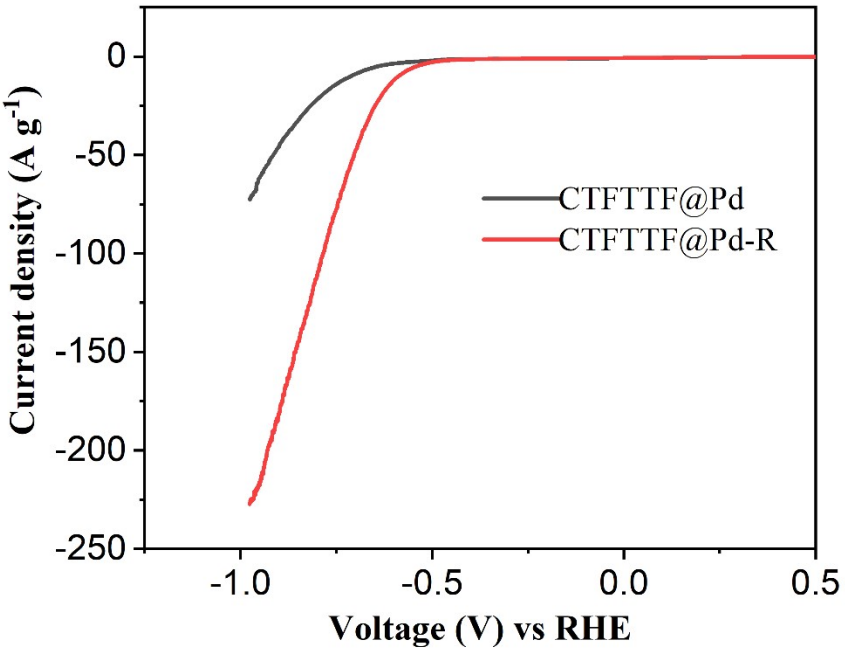

Fig. S21: LSV plots to represent the mass activity (A/g).

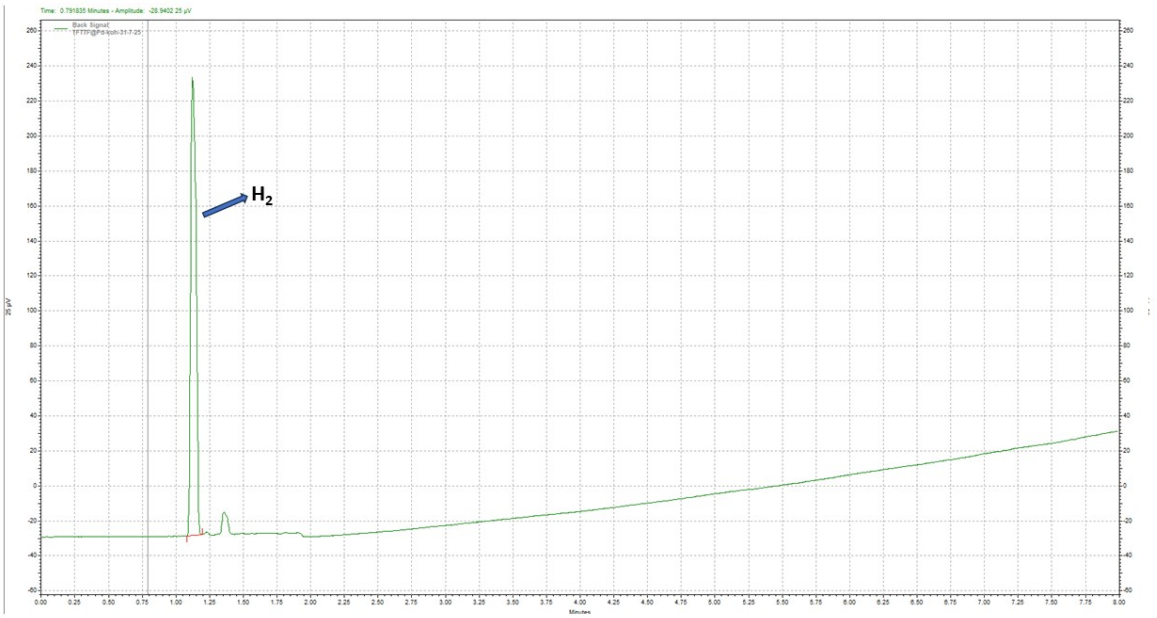

Fig. S22: Gas Chromatography data after HER.

Reference

1. A. Maity, A. Jana, S. Kumar Dey, C. Janiak and A. Bhunia, *Mater. Adv*., 2025, **6**, 4337-4344.

2. D. Kaleeswaran, R. Antony, A. Sharma, A. Malani and R. Murugavel, *Chempluschem,* 2017, **82**, 1253–1265.

3. I. Romero-Mu˜ niz, A. Mavrandonakis, P. Albacete, A. Vega, V. Briois, F. Zamora and A. E. Platero-Prats, *Angew. Chem. Int. Ed.,* 2020, **132**, 13113–13120.

4. Y. Li, B. Pei, J. Chen, S. Bing, L. Hou, Q. Sun, G. Xu, Z. Yao and L. Zhang, *J. Colloid Interface Sci.*, 2021, **591**, 273–280.

5. J. Liu, H. Zhan, N. Wang, Y. Song, C. Wang, X. Wang, L. Ma and L. Chen, *ACS Appl.*

Nano Mater., 2021, **4**, 6239–6249.

6. I. Romero-Muñiz, A. Mavrandonakis, P. Albacete, A. Vega, V. Briois, F. Zamora, A. E. Platero-Prats, *Angew. Chem*, 2020, **59**, 13013-130020.

7. J. Kouhdareh, H. Keypour, S. Alavinia, A. Maryamabadi, *Journal of Molecular Structure*, 2023, **1273**, 134286.

8. J.-C. Wang, C.-X. Liu, X. Kan, X.-W. Wu, J.-L. Kana and Y.-B. Dong, *Green Chem.,* 2020, **22**, 1150-1155.

9. S. Y. Ding, J. Gao, Q. Wang, Y. Zhang, W. G. Song, C. Y. Su and W. Wang, *J. Am. Chem. Soc.,* 2011, **133**, 19816–19822.

10. S. Lu, Y. Hu, S. Wan, R. McCaffrey, Y. Jin, H. Gu and W. Zhang, *J. Am. Chem. Soc.,* 2017, **139**, 17082–17088.

11. Q. Sun, C. Wu, Q. Pan, B. Zhang, Y. Liu, X. Lu, J. Sun, L. Sun and Y. Zhao, *ChemNanoMat*, 2021, **7**, 95–99.

12. J.-Y. Yue, X.-L. Ding, L.-P. Song, Y.-T. Wang, P. Yang, Y. Ma, B. Tang, *Microporous Mesoporous Mater*., 2022, **344**, 112169.

13. Y. Sun, J. Lee, H. Kwon, J. Lim, X. Jin, Y. Gogotsi and S.-J. Hwang, *ACS Nano 2024*, **18**, 6243–6255.

14. T. Bhowmik, M. K. Kundu and S. Barman, *ACS Catal*., 2016, **6,** 1929.

15. M. Woldetinsay, T. R Soreta, T. Maiyalagan and O. E. Femi, *Mater. Res. Express*, 2021, **8**, 025501.

16. Y. Fang, X.-Y. Yu, X. W. Lou, *Matt.,* 2019, **1**, 90-114.

17. Y.C. Shi, J.J. Feng, X.X. Lin, L. Zhang, J.H. Yuan, Q.L. Zhang, A.J. Wang, *Electrochim. Acta*, 2019, **293**, 504-513.

18. R. V. Hegde, R. Bhondwe, K. A. Sree Raj, A. Ghosh, C. S. Rout, R. Thrilokraj, S. A. Patil, B. Sridhar and R. B. Dateer, *ChemistrySelect*, 2023, **8**, e202300673.

19. N. Wang, B. Tao, F. Miao, Yu Zangb, *RSC Adv*., 2019, **9**, 33814-33822.

20. H. Liu, J. Shang, L. Zeng, B. Cao, H. Geng, J. Lang, X. Cao, H. Gu, Chem. Eng. *J. Adv.*, 2021, **6**, 100101.

21. S. Sarkar and S. Sampath, *Chem. Commun.*, 2014, **50**, 7359 —7362.

22. P. Chandrasekaran, T.N. Jebakumar Immanuel Edison, M.G. Sethuraman, *Int. J. Hydrogen Energy*, 2020, **45**, 28800-28811.

23. C. Taechaworaphong, M. Juthathan, P. Thamyongkit, T. Tuntulani and P. Leeladee,

ChemPlusChem, 2024, **89**, e202300679.

24. R. Samanta, B. K. Manna, R. Trivedi, B. Chakraborty, and S. Barman, *Chem. Sci*., 2024, **15**, 364.

25. V. Vishwakarma, N. Diyali, A. De, A. R. Choudhury and B. Biswas, *ChemPlusChem*, 2025, **90**, e202500177.

26. M. Pal,a R. Biswas, S. Barman and A. Dutta *Energy Adv*., 2024, **3**, 1562-1570.